CIRP Journal of Manufacturing Science and Technology 30 (2020) 58–67

Contents lists available at ScienceDirect

CIRP Journal of Manufacturing Science and Technology

journal homepage: www.elsevier.com/locate/cirpj

Modulated vibration texturing of hierarchical microchannels with controllable profiles and orientations

Jianjian Wang[a,b], Ru Yang[a], Shiming Gao[b], Fei Weng[b], Yaoke Wang[a], Wei-Hsin Liao[b], Ping Guo[a,*]

[a] Department of Mechanical Engineering, Northwestern University, Evanston, IL, USA
[b] Department of Mechanical and Automation Engineering, The Chinese University of Hong Kong, Shatin, Hong Kong, China

ARTICLE INFO

Article history:
Available online 20 May 2020

Keywords:
Hierarchical structure
Microchannel
Elliptical vibration cutting
Surface texturing

ABSTRACT

Hierarchical microchannels, which consist of the primary channel formation and superimposed secondary nanostructures, are attracting ever-increasing attention due to their unique capacity to enhance and modify the surface characteristics and functional performance. The mechanical machining methods for microchannel fabrication, such as micro-milling and diamond turning, can achieve high material removal rates without changing material properties. However, they have limited capacity to control the channel cross-section profiles and shapes due to the relative size between the channel dimension and tool geometry. This study proposes a new cutting-based approach for the fast and cost-effective fabrication of hierarchical microchannels with controllable profiles and orientations by utilizing modulated elliptical vibration texturing. The modulation motion is adopted to form the primary channel in an incremental approach, while the elliptical vibration texturing is utilized to create micro/nano-scale secondary textures. By controlling the tool modulation trajectory, hierarchical dimple arrays with controllable cross-section profiles are first demonstrated. Then, by programming the layout of dimples to adjust the overlapping ratio between each cut, channels can be formed with arbitrary cross-section profiles and orientations. The efficacy of the proposed process has been demonstrated through numerical simulation and experimental results. Hierarchical microchannels with straight and curving shapes, as well as different cross-section profiles (sinusoidal, triangular, trapezoidal), have been presented.

Introduction

Hierarchical microchannels consist of the primary channel formation and superimposed secondary nanostructures. Various creatures widely adopt them in nature for spontaneously tuning of their skin properties, such as adhesion, wettability, and optical response. With the utilization of hierarchical channels, various specific bio-functions are achieved to assist creatures in combating and surviving with the continuously changing environment [1]. For example, as shown in Fig. 1, sarracenia trichome utilizes hierarchical microchannels to achieve ultrafast water harvesting from surrounding fog to wet the slippery-footing peristome surface for insects catching [2]. Inspired by nature, various kinds of artificial hierarchical channels have been used to achieve unique surface properties, such as directional liquid transport [3], anisotropic wettability [4], drag/friction reduction [5].

Many kinds of non-mechanical and mechanical micro/nano-manufacturing methods have been introduced for the fabrication of hierarchical microchannels. The non-mechanical methods mainly include lithography, direct laser patterning, chemical/electrochemical etching, etc. Lithography-based processes are dominant in the fabrication of microchannel patterns [6]. However, as a laborious multi-step process to generate super-imposed secondary nanostructures, the lithography suffers from low efficiency. It is also challenging for lithography to control the cross-section profile of hierarchical channels. Laser interference patterning can be applied to fabricate hierarchical channels on various kinds of materials, but the surface quality of laser patterned structures is shallow due to the heating induced material fusion [7]. Chemical or electrochemical etching is usually applied to create hierarchical structures on metal surfaces for the wettability modification, but it is not well-received in the modern industry due to the utilization of environment-unfriendly chemical etchants [8].

Compared with the non-mechanical methods, due to their physical-based material removal principle, the mechanical machining methods are promising to fabricate hierarchical channels

* Corresponding author.
E-mail addresses: wangjj11@outlook.com, jjwang@northwestern.edu (J. Wang), ping.guo@northwestern.edu (P. Guo).

https://doi.org/10.1016/j.cirpj.2020.04.002
1755-5817/

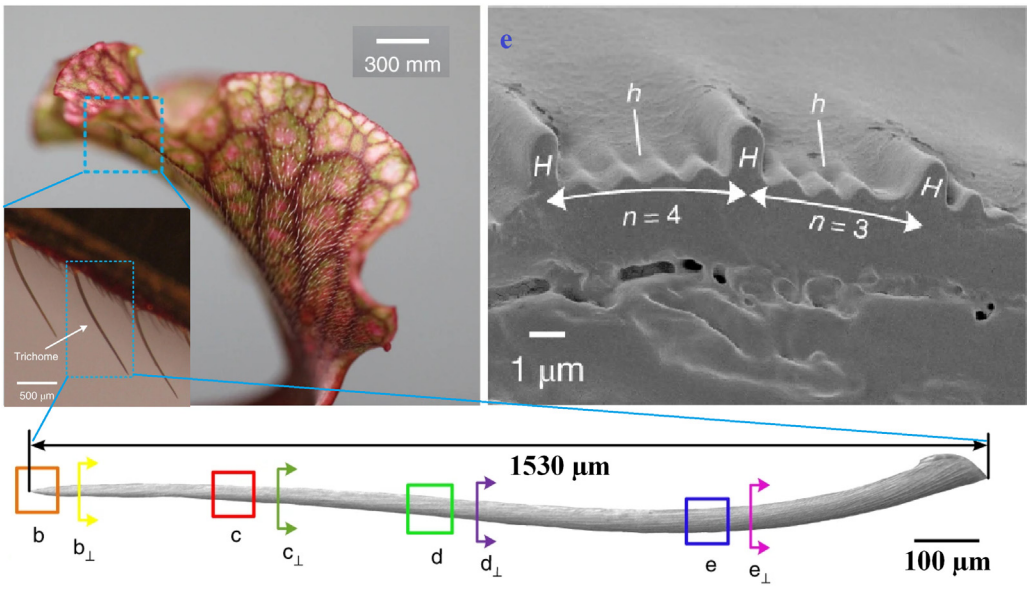

Fig. 1. Images of hierarchical channels on sarracenia trichome [2].

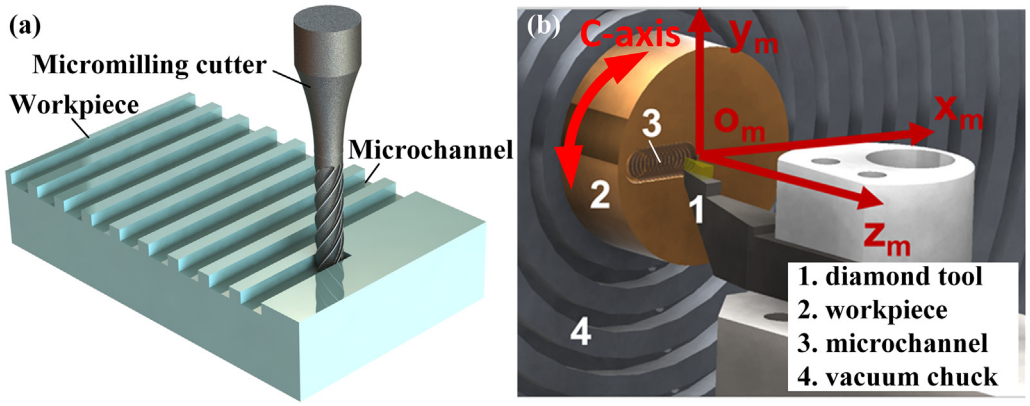

Fig. 2. Illustration of microchannel fabrication by (a) micro-milling and (b) diamond turning [11].

with higher efficiency, accuracy, and surface quality, without changing the original material properties. The mechanical machining methods for microchannel fabrication mainly consist of groove ruling, micro-milling, and diamond turning. Groove ruling is the most widely applied technique for the fabrication of microchannels. However, the microchannels fabricated by ruling are usually restricted to straight channels with fixed cross-section profiles. Micro-milling, which utilizes a high-speed rotational micro cutter to remove materials with small chips, as shown in Fig. 2(a), has multiplied in recent years to fabricate microchannels on metal and polymers with feature size down to 10 μm in the field of microfluidic devices [9]. However, due to its intrinsic kinematics, micro-milling has limited capacity to create secondary nano-structures on the generated primary microchannel [10]. Besides, the minimal achievable width and cross-sectional profile are limited by the tool radius and shape. One has to compromise the design flexibility of microchannel profiles to the available tool geometry to keep down the manufacturing cost. In order to overcome the above restriction of micro-milling, Zhu et al. proposed a tool path modulation method to adopt slow slide servo and diamond turning for the fabrication hierarchical channels, as shown in Fig. 2(b) [11]. However, due to the limited dynamic bandwidth of slow slide servo, the method still suffers from a low production rate. Moreover, the tool path modulation method converts rotational motion into translational channel formation, which adds more complexity and difficulty for industrial implementation.

To address the research gaps discussed above, this study proposes a novel mechanical machining approach for the fast fabrication of hierarchical microchannels based on a modulated elliptical vibration texturing process. The modulated elliptical vibration texturing process, which combines the tool modulation cutting and elliptical vibration texturing with a 2-D ultrafast non-resonant tool, is utilized to generate hierarchical dimple patterns on metallic surfaces in one step. By programming the overlapping of hierarchical dimples, the hierarchical channels with controllable orientations can be formed. In the meantime, the cross-section profile of hierarchical channels can also be tuned by the tool modulation trajectory. The machining efficiency can be enhanced with the high-frequency bandwidth of the utilized vibration cutting tool. Overall, the proposed new approach shows improved efficiency as well as flexibility in terms of the control of cross-section profiles and orientations over the existing methods (micro-milling and diamond turning).

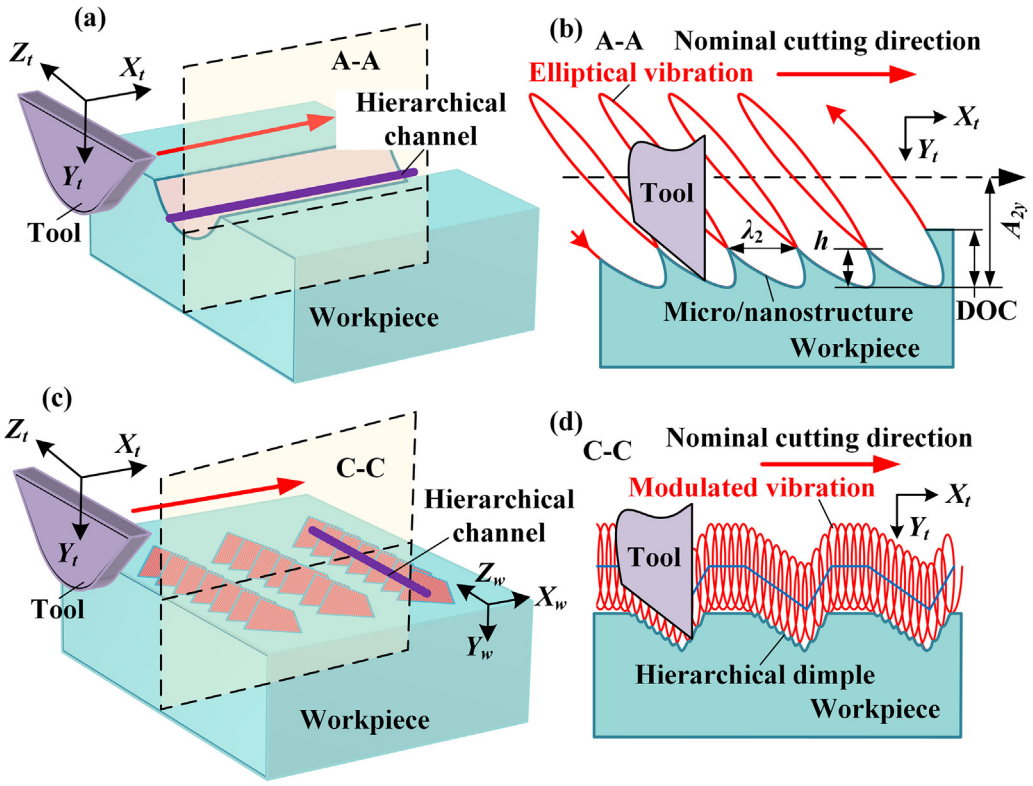

Fig. 3. Proposed generation principle of hierarchical channels. (a and b) Elliptical vibration texturing; (c and d) modulated vibration texturing.

Hierarchical structures generation principle

Principle of modulated elliptical vibration texturing

Modulated elliptical vibration texturing combines the tool modulation cutting and elliptical vibration texturing. In elliptical vibration texturing, through its unique overlapping tool trajectory, conjunct micro/nano-grooves can be created at the rate of vibration frequency (several hundred hertz to 40 kHz). As shown in Fig. 3(a) and (b), elliptical vibration texturing can be applied in a ruling configuration for the direct fabrication of hierarchical microchannels. Compared with diamond turning, it has improved fabrication efficiency. However, direct elliptical vibration texturing still has the drawbacks of low process flexibility: 1) the cross-section profile of microchannel is hardly adjustable due to the direct replication of the tool geometry. 2) The channel orientation is not adjustable due to the restriction of the singular cutting direction. 3) The relative orientation of superimposed secondary nanostructures with respect to the primary channel is fixed, due to the restriction of fixed elliptical vibration direction.

Through the addition of tool modulation motion on elliptical vibration texturing, the process flexibility can be significantly improved while maintaining its advantages of high efficiency. In the newly proposed modulated elliptical vibration texturing, as shown in Fig. 3(c) and (d), a low-frequency modulation motion is added to the high-frequency elliptical vibration in the depth-of-cut (DOC) direction. A similar approach of modulated elliptical vibration texturing has been used to fabricate microstructures on difficult-to-cut materials [12,13], which utilizes elliptical vibration to improve material machinability [14,15]. However, in this study, the elliptical vibration is leveraged to generate superimposed secondary nanostructures on the primary microchannels. By effectively cutting the channel in the oblique direction, the channels are machined in segments. As shown in Fig. 3(c), the channel orientation and shape can be adjusted by tool path planning, while the secondary feature direction can be adjusted by tuning the relative angle between the channel formation and cutting direction. Also, the cross-section profile is de-coupled from tool geometry but relies on modulation trajectory, which can be dynamically adjusted, as shown in Fig. 3(d).

The tool kinematics determine the geometries of generated hierarchical structures. In order to describe the tool kinematics, two coordinate systems are defined in Fig. 3(c). The workpiece coordinate system ($O_wX_wY_wZ_w$) is attached to the workpiece surface. The tool coordinate system ($O_tX_tY_tZ_t$) is established on the nose center of the tool rake, assuming an indexable turning insert. X_w and X_t are in the cutting direction; Y_w and Y_t are in the DOC direction; Z_w and Z_t are in the feed direction. The resultant tool motion in modulated vibration texturing consists of three motion components: the nominal cutting, the low-frequency modulation, and the high-frequency elliptical vibration. The overall tool motion with respect to the workpiece can be expressed in the tool coordinate system ($O_tX_tY_tZ_t$) as,

$$\begin{cases} X_m(t) = v_c t + \boxed{A_{2x}\sin(2\pi f_2 t)} \cdots\cdots u_x \\ Y_m(t) = \boxed{A_{1y}g(2\pi f_1 t) + A_{2y}\sin(2\pi f_2 t + \varphi)} \cdots\cdots u_y \\ Z_m(t) = feed \cdot k \cdot True\left[(k-1)T_x < t \le kT_x\right], k = 1,2,\cdots \end{cases} \quad (1)$$

where X_m,Y_m, Z_m are the tool motion in the X_t-, Y_t-, Z_t-directions, respectively. t denotes time. v_c is the nominal cutting speed. *feed* refers to the cross-feed distance. T_x is the total time of one cutting pass in X_t direction. For the two-level tool modulation motion, f_1 and A_{1y} are the frequency and amplitude of modulation motion (low-frequency). g is a function to describe the modulation motion, which might be a non-harmonic periodic trajectory. f_2, A_{2x}, A_{2y}, φ are the frequency, amplitudes, and phase of elliptical vibration (high-frequency). The three levels of tool motions are provided by

different sources. To be specific, the nominal cutting motions are provided by the machine tool motion stages. The modulation motion (low-frequency) and elliptical vibration (high-frequency) are both provided by a piezo-actuated 2-D non-resonant tool. The combined modulated elliptical vibration motions provided by the 2-D non-resonant tool are in the cutting and DOC directions, which are denoted by u_x and u_y in Eq. (1).

One-step machining of hierarchical dimples with controllable cross-section profile

Hierarchical dimple is the basic structural unit that the proposed modulated vibration texturing can fabricate. The primary and secondary structures of a hierarchical dimple are the micro-dimple and micro/nano-grooves, which can be generated by the tool modulation and elliptical vibration, respectively.

Hierarchical dimple patterns with controllable geometric parameters can be generated by adjusting the process parameters. The derivation of hierarchical dimple geometry is shown in Fig. 4. The geometric parameters of the primary structure include the primary interval λ_1, width w, depth DOC, and length l. The geometric parameters of the secondary structure include the secondary interval λ_2, and depth h. The relationship between the hierarchical dimple geometries and process inputs of modulated vibration texturing can be expressed as,

$$\begin{cases} \lambda_i = v_c/f_i (i = 1,2) \\ w = 2\sqrt{R^2 - (R - \mathrm{DOC})^2} \\ l = v_c \cdot \Delta t \\ h = A_{2y}(1 - \sin(2\pi f_2 t_0 + \varphi)) \end{cases} \tag{2}$$

where Δt is the actual cutting time in one modulation period, which can be calculated from modulation motion $g(t)$ and DOC. t_0 is an intermediate variable of time, which can be obtained by solving the following equations.

$$\begin{cases} A_{2x}\sin(2\pi f_2 t_0) + v_c t_0 = A_{2x}\sin(2\pi f_2 t'_0) + v_c t'_0 \\ 2\pi f_2 (t_0 + t'_0) + 2\varphi = 3\pi \end{cases} \tag{3}$$

Generation of hierarchical channels by programming the layout of hierarchical dimples

Channel arrays can be formed by programming the layout of hierarchical dimples to control the overlapping of neighboring dimples. The layout parameters of hierarchical dimples consist of phase-shift distance δ and feed distance *feed*, as shown in Fig. 5(a). When *feed* is small enough, neighboring dimples can overlap with each other to form a channel. The horizontal distance d_O between the boundary of neighboring dimples can be expressed as Eq. (4), which indicates that the overlapping is determined by the tool nose radius, feed distance, and DOC. To generate hierarchical microchannels with continuous boundary formation, a larger tool nose radius, a larger DOC, or a smaller feed distance is beneficial. Also, the phase-shift distance δ influences the overlapping of neighboring dimples. With a relatively large phase-shift distance δ, the maximal allowable values for tool nose radius, DOC and feed distance has to be further confined.

$$d_O = feed - 2\sqrt{R^2 - (R - \mathrm{DOC})^2} \tag{4}$$

The proposed process shows high flexibility for the control of cross-section profiles. The cross-section profile can be tuned through the design of modulation motion function $g(t)$. If $g(t)$ has the definition of a sinusoidal, triangular, or trapezoidal function, the formed channels will have the corresponding cross-section profiles. Moreover, the channel orientation can be controlled as well. The channel orientation angle θ_r, as defined in Fig. 5(a), can be controlled by the feed distance *feed* and phase-

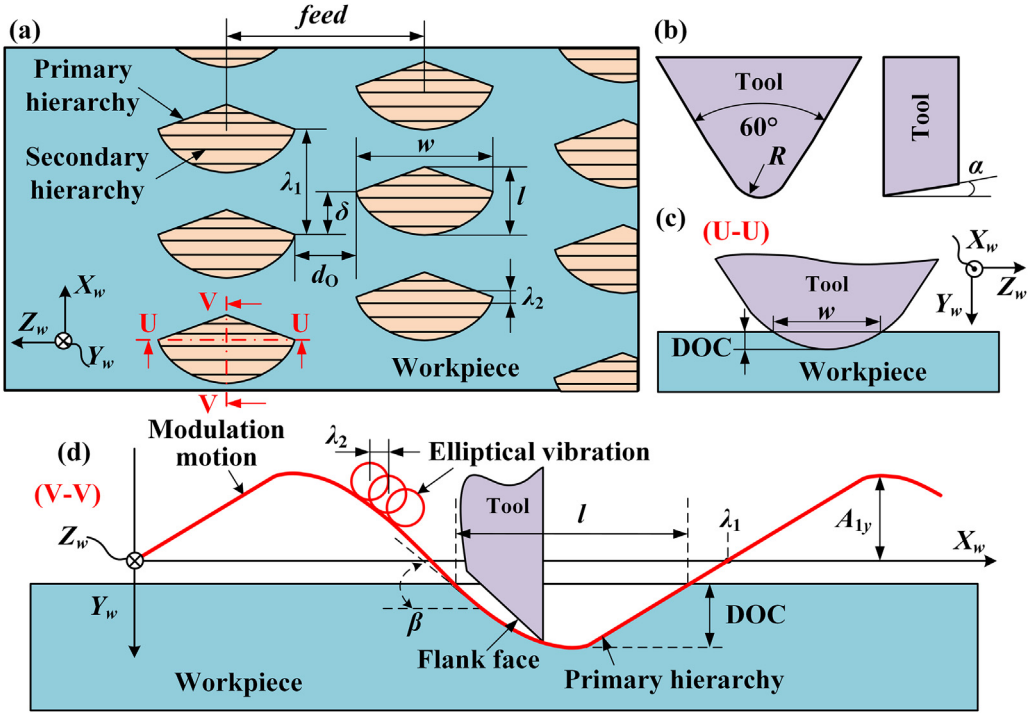

Fig. 4. Geometry configuration of hierarchical dimples. (a) Dimple layout; (b) geometric parameters of the diamond tool; (c) relationship between the depth of cut and cutting width; (d) calculation of the dimple length.

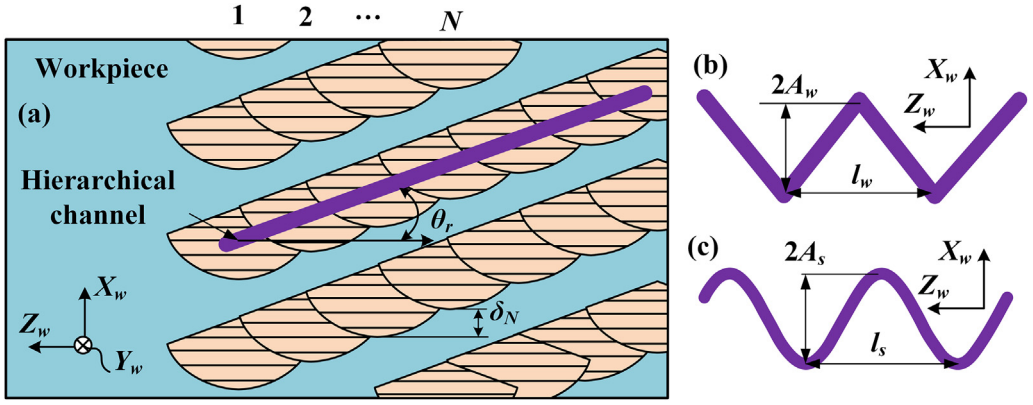

Fig. 5. (a) Generation principle of hierarchical channel patterns; top view of the schematic of (b) zigzag and (c) wiggling channels.

shift distance δ as,

$$\theta_r = arctan\left(\frac{\delta}{feed}\right) \tag{5}$$

$\delta = 0$ corresponds to the horizontal straight channel formation. When δ is set to non-zero, oblique channels can be machined with different orientations. Curving channels can also be fabricated if the phase-shift distance δ is set to a variable δ_N based on the index number N. In particular, we demonstrated the cases of generating zigzag and wiggling channels as shown in Fig. 5(b) and (c). δ_N is defined according to the wavelength l_w (l_s) and amplitude A_w (A_s) of the zigzag (wiggling) channels through Eqs. (6) and (7) respectively.

$$\delta_N = \begin{cases} A_w \cdot \frac{2\pi}{l_w} \cdot feed, & 0 < N \le \frac{l_w}{2feed} \\ -A_w \cdot \frac{2\pi}{l_w} \cdot feed, & \frac{l_w}{2feed} < N < \frac{l_w}{feed} \end{cases} \tag{6}$$

$$\delta_N = A_s\left(\sin\left(\frac{2\pi}{l_s} \cdot feed \cdot N\right) - \sin\left(\frac{2\pi}{l_s} \cdot feed \cdot (N-1)\right)\right) \tag{7}$$

Experimental setup and methods

Surface texturing experiments were conducted to verify the efficacy of the proposed modulated vibration texturing process. Three kinds of hierarchical structures are generated with their optical images shown in Fig. 6, including (i) hierarchical dimples with sinusoidal, triangular, and trapezoidal cross-section profiles; (ii) hierarchical straight channels with sinusoidal, triangular, and trapezoidal cross-section profiles; (iii) curving hierarchical channels with zigzag and sinusoidal orientations. The optical images of machined surfaces are shown in Fig. 6. The surfaces present iridescent color. This color comes from light diffraction on the periodic secondary microstructures. Though the structural coloration is not the target application of fabricated hierarchical structures, the presented iridescent colors can help to indicate the successful generation of secondary structures.

An ultrafast 2-D non-resonant tool is used to provide modulation motion and elliptical vibration simultaneously in this study. The design of the vibration cutting tool is illustrated in Fig. 7(a), where two piezo stack actuators are used to generate two-directional motions, and then bridge-type displacement amplifiers are used to magnify the motions from actuators. Due to its unique compact design, the 2-D non-resonant tool has a full stroke of 9.5 μm × 15 μm, and a frequency bandwidth of up to 6 kHz. The structural dynamics of the ultrafast tool have been presented in our previous study [16]. The first resonant frequency of the tool is above 6 kHz, which results in a good linear response in the whole frequency bandwidth. This enables the precise control of tool trajectories in a continuous frequency range. In addition to harmonic elliptical vibrations, the developed tool is able to generate non-harmonic trajectories, which can be used to provide modulation motion in this study. On the one hand, to ensure the accurate trajectory generation of modulation motion, the Fourier series of the non-harmonic periodic excitation signals should have as many orders of frequency contents as possible. On the other hand, the highest frequency order should not exceed the tool bandwidth. The non-harmonic excitation signal is usually set below one-twentieth of the first natural frequency, which gives a usable frequency bandwidth up to 300 Hz for this tool. This bandwidth also largely depends on the complexity of the non-harmonic trajectory.

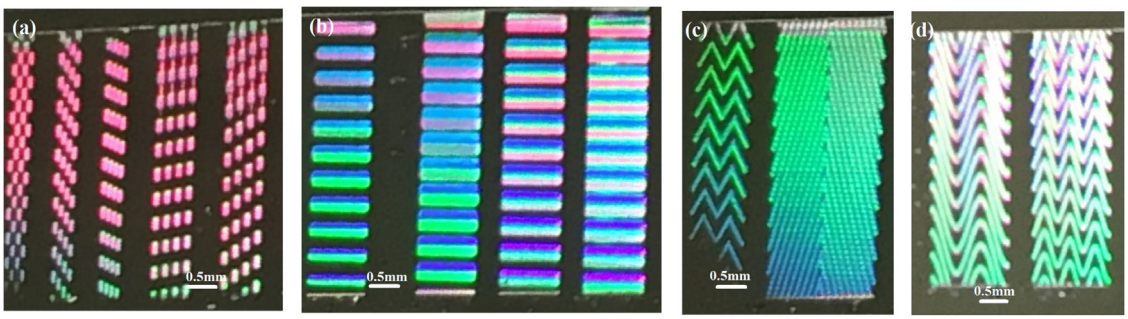

Fig. 6. Optical image of generated hierarchical structures with iridescent effects. (a) Hierarchical dimples; (b) hierarchical straight channels; (c and d) hierarchical curving channels with zigzag and sinusoidal orientations.

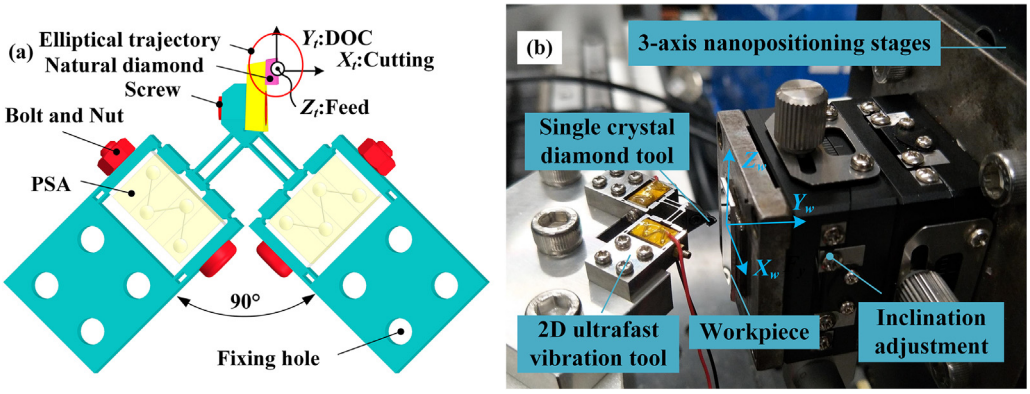

Fig. 7. Surface texturing setup. (a) 2-D ultrafast vibration tool [16] and (b) experimental setup.

Table 1
Process conditions of surface texturing of aluminum alloy.

No.	Feed (μm)	Cutting speed	Elliptical vibration	Modulation motion
1	25, 75, 100, 200	9 mm/s	3000 Hz	Sine, 20 Hz and 60 Hz
2	25, 75, 100, 200	9 mm/s	3000 Hz	Triangle, 20 Hz and 60 Hz
3	25, 75, 100, 200	9 mm/s	3000 Hz	Trapezoid, 20 Hz and 60 Hz

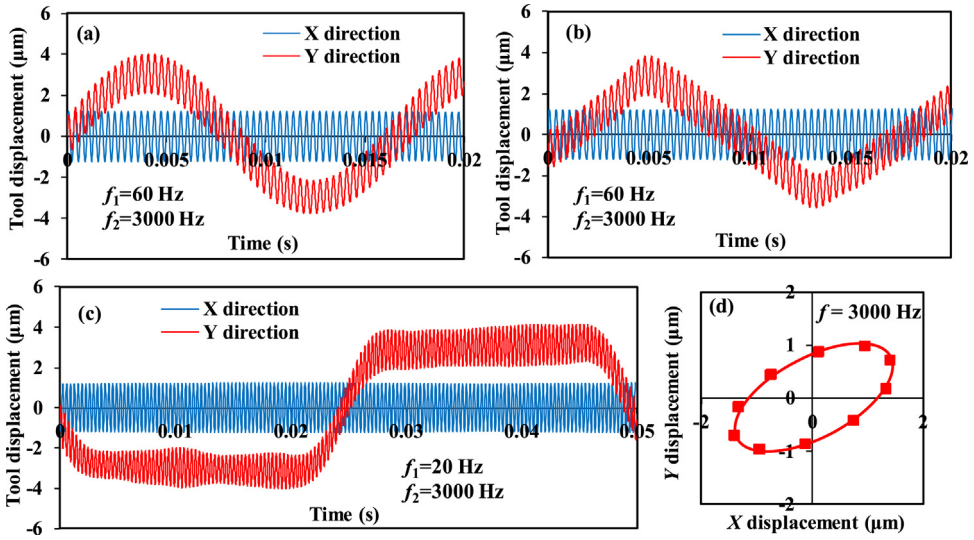

Fig. 8. Measured results of (a) sinusoidal, (b) triangular, and (c) trapezoidal modulated elliptical vibration trajectories and (d) original elliptical trajectory.

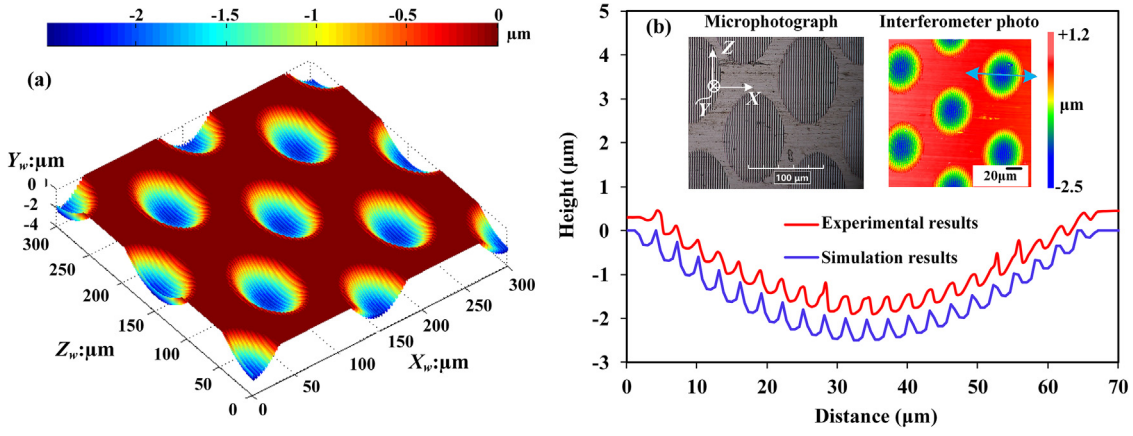

Fig. 9. Generated hierarchical dimples with a sinusoidal profile. (a) Simulated results and (b) experimental results.

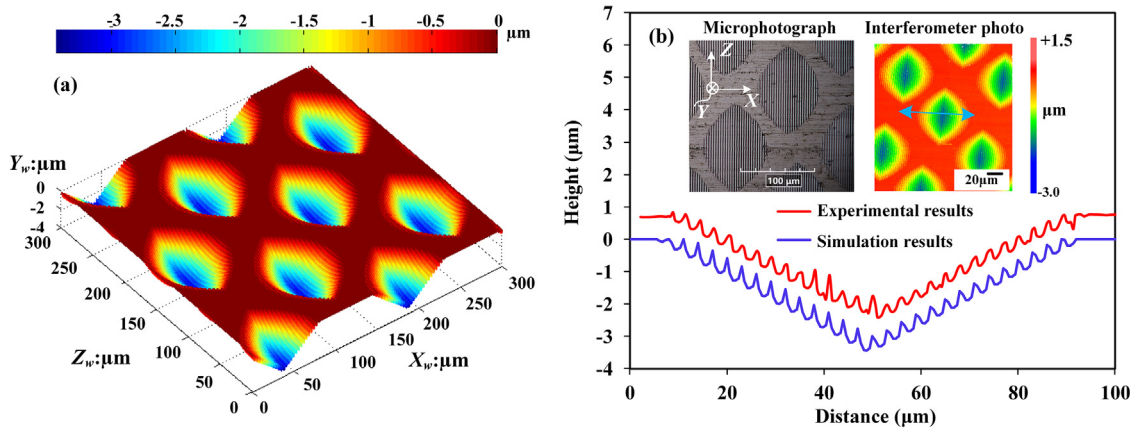

Fig. 10. Generated hierarchical dimples with a triangular profile. (a) Simulated results and (b) experimental results.

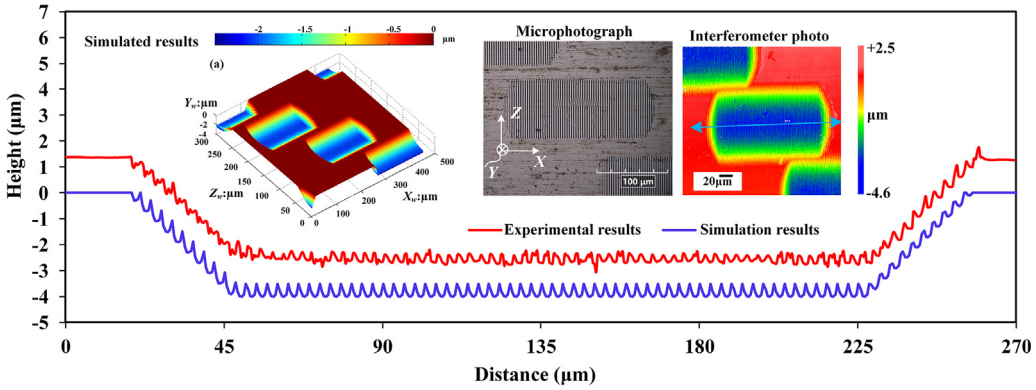

Fig. 11. Generated hierarchical dimples with a trapezoidal profile.

The generation trajectories of modulated elliptical vibration using the 2-D vibration tool can be described by:

$$\begin{bmatrix} u_x(t) \\ u_y(t) \end{bmatrix} = \begin{bmatrix} A_x & -A_x \\ A_y & A_y \end{bmatrix} \begin{bmatrix} U_L(t) = U_1(f_1,t) + U_{2L}\sin(2\pi f_2 t) \\ U_R(t) = U_1(f_1,t) + U_{2R}\sin(2\pi f_2 t + \phi) \end{bmatrix} \tag{8}$$

where U_L and U_R are the input voltages of two piezo stacks, respectively. A_x and A_y are the coefficients that transform input voltages to output displacement. U_1 describes the input voltage to provide modulation motion. U_{2L}, U_{2R}, are the amplitudes and phase differences of input voltages to generate elliptical vibration.

The experimental setup is shown in Fig. 7(b). The 2-D non-resonant tool is mounted on a direct-drive linear actuator (ACT165DL, *Aerotech, USA*), which is utilized to generate the nominal cutting motion along the *X*-direction relative to the workpiece. The aluminum alloy workpiece with a dimension of 2 mm × 10 mm × 30 mm was glued to a two-degree-of-freedom tilt stage, which could be used for inclination adjustment. The tilt stage is mounted on a three-axis nanopositioning stage (ANT130XY and ANT130LZ, *Aerotech, USA*), which is used to generate relative feed motion. A natural single crystal diamond cutter (*Contour Fine Tooling, UK*) with a nose radius of 500 μm, a rake angle of 0°, and a clearance angle of 10° was used for cutting. A digital camera was used for tool setting. The critical processing parameters with sinusoidal, triangular, and trapezoidal waveform modulation motions are listed in Table 1. The modulated vibration trajectories were measured using a pair of capacitance displacement sensors before actual texturing, which are plotted in Fig. 8. The obtained structured surfaces were measured using a digital microscope (RH-2000, Hirox) and an optical surface profiler (Zygo).

Numerical simulation is conducted to preliminarily verify the feasibility of hierarchical microchannel formation and to validate the process parameters before the texturing experiments. The numerical simulation is based on the description of tool kinematics, which is described by Eq. (1) in section "Hierarchical structures generation principle", as well as the tool geometries. Due to the relative motion between tool and workpiece, the interactions of the tool's rake, cutting edge, and flank face with the workpiece meshes define the material removal in the simulation procedure. Detailed information about the numerical simulation procedure can be found in our previous study [17].

Results and discussion

Basic structural unit: hierarchical dimples

Hierarchical dimples with sinusoidal, triangular, and trapezoidal cross-section profiles have been experimentally generated respectively along with the numerical simulation results shown in Figs. 9–11. The cross-section profiles of the dimples can be dynamically adjusted through the tool modulation trajectory. As shown in Figs. 9–11, every single dimple consists of two-level structures: the primary dimple profile and the secondary micro/nano-textures. The primary structure is a general micro-dimple with different cross-section profiles, while the secondary textures are parallel grooves with an interval distance of three micrometers and the height of several hundred nanometers. These structural parameters are determined by the combination of cutting parameters, particularly the tool vibration frequencies and amplitudes. The numerical simulation results of the cross-section profiles of hierarchical dimples agree well with the experimental

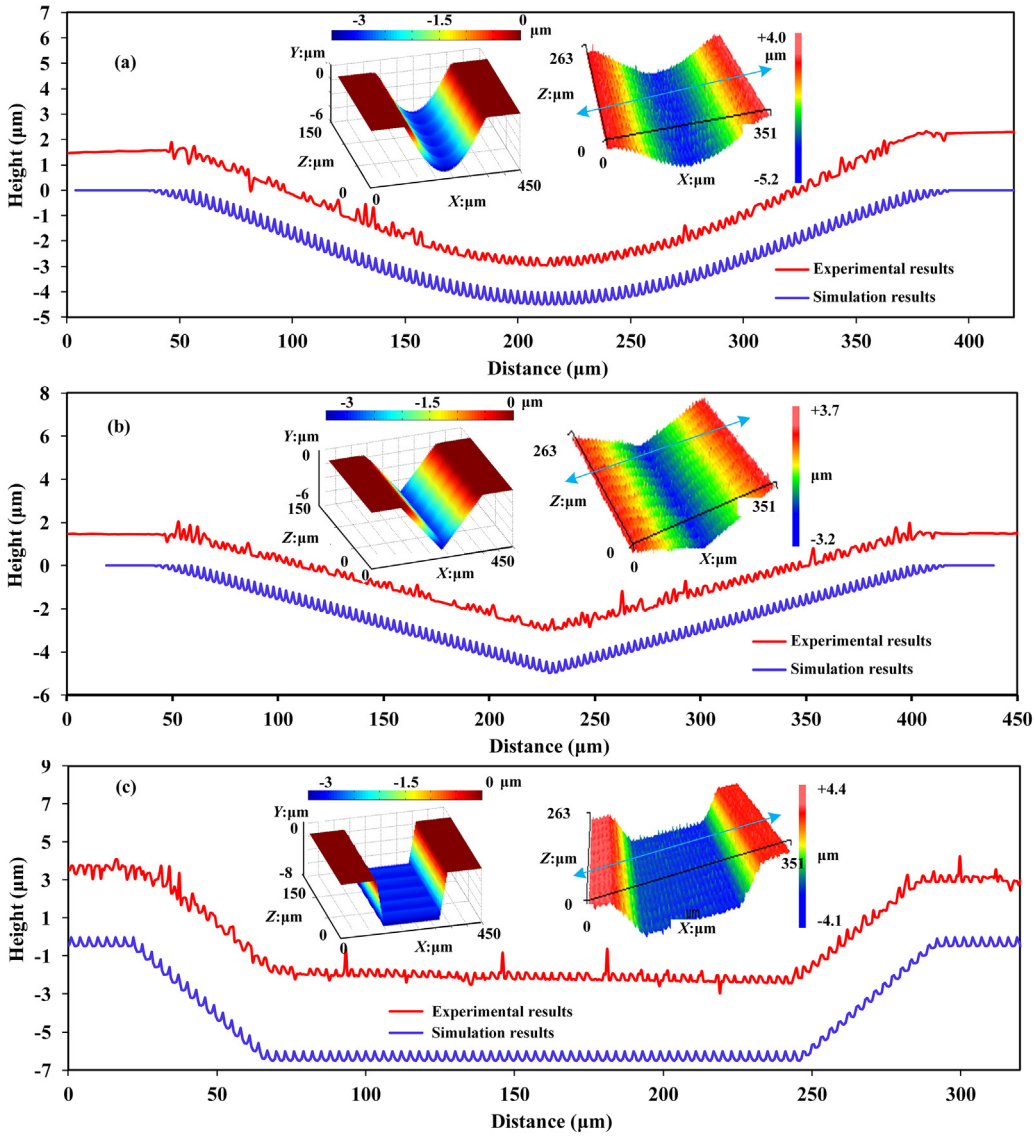

Fig. 12. Surface topography and profiles of generated hierarchical channels with controllable cross-section profiles. (a) Sinusoidal profile; (b) triangular profile; (c) trapezoidal profile.

results, which demonstrates that the numerical simulation can be applied in the process parameters determination to study the hierarchical structure formation.

Hierarchical channels with controllable cross-section profile

By tuning the layout of generated hierarchical dimples, hierarchical channels with a controllable cross-section profile can be fabricated efficiently. Through the design of tool modulation trajectories, the microchannel cross-section profile can be decoupled from the tool geometry. Hierarchical straight channels with various kinds of cross-section profiles have been fabricated by setting the phase-shift distance $\delta = 0$. Fig. 12 shows the experimental and numerical results of hierarchical straight channels with sinusoidal, triangular, and trapezoidal cross-section profiles. The numerical simulation results of the microchannel profile are consistent with the experimental results. The successful fabrication of hierarchical microchannels with different cross-section profile confirms the capacity of proposed modulated vibration texturing in the cross-section profile control.

Hierarchical curving channels with controllable orientations

The orientation of hierarchical microchannels can also be controlled by the overlapping layout of machined dimples. In particular, the orientation of primary microchannel can be adjusted by tool path planning, while the secondary nanostructures direction can be tuned through the relative angle between the channel formation and nominal cutting direction. Hierarchical oblique channels have been fabricated by keeping the phase-shift distance δ as a non-zero value. The experimental results are shown in Fig. 13, which demonstrates that the effect of phase-shift distance on the channel formation. The fabricated straight microchannels (Fig. 13(b)) with as small as zero phase-shift distance, have much smoother boundaries than the oblique microchannels (Fig. 13(a) and (c)) with non-zero phase-shift distance. To improve the profile smoothness of oblique microchannels with a non-zero shift distance, a reduced feed distance is recommended. The above results verify the capacity of the proposed process in the fabrication of hierarchical microchannels with controllable orientations.

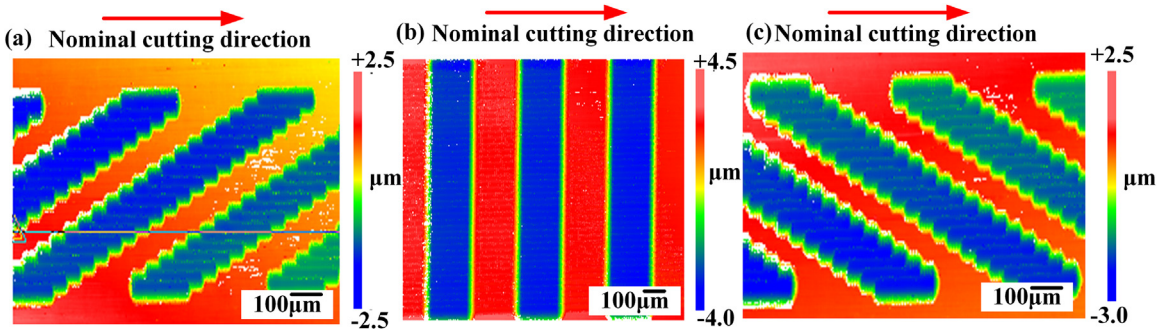

Fig. 13. Interfere photo of generated hierarchical channels (*feed* = 25 μm). (a) left-oblique channel when $\delta < 0$; (b) straight channel when $\delta = 0$; (c) right-oblique channels when $\delta > 0$.

Hierarchical curving channels with spatial-varying orientations have also been fabricated by controllably adjusting the phase-shift distance δ_N in Eqs. (5) and (6). Fig. 14 shows the surface morphology of generated hierarchical curving channels. When the δ_N follows the relationship with cutting passes defined in Eq. (5), zigzag curving hierarchical channels can be fabricated as shown in Fig. 14(a) and (b). On the other hand, when the δ_N follows the relationship with cutting passes defined in Eq. (6), wiggling curving hierarchical microchannels can be fabricated, as shown in Fig. 14(c) and (d). The results in Fig. 14 further verify the capacity of proposed texturing method in the orientation control of generated hierarchical microchannels.

The results in Fig. 14 also demonstrate the effects of process parameters (DOC and phase-shift distance) on the overlapping of neighboring dimples. A larger DOC and smaller phase-shift distance benefit the overlapping of neighboring dimples. By comparing Fig. 14(a) and (b) and Fig. 14(c) and (d), we can find that the boundary of the wiggling microchannels is smoother than that of the zigzag microchannels. The better smoothness of wiggling microchannel can be attributed to the larger dimple

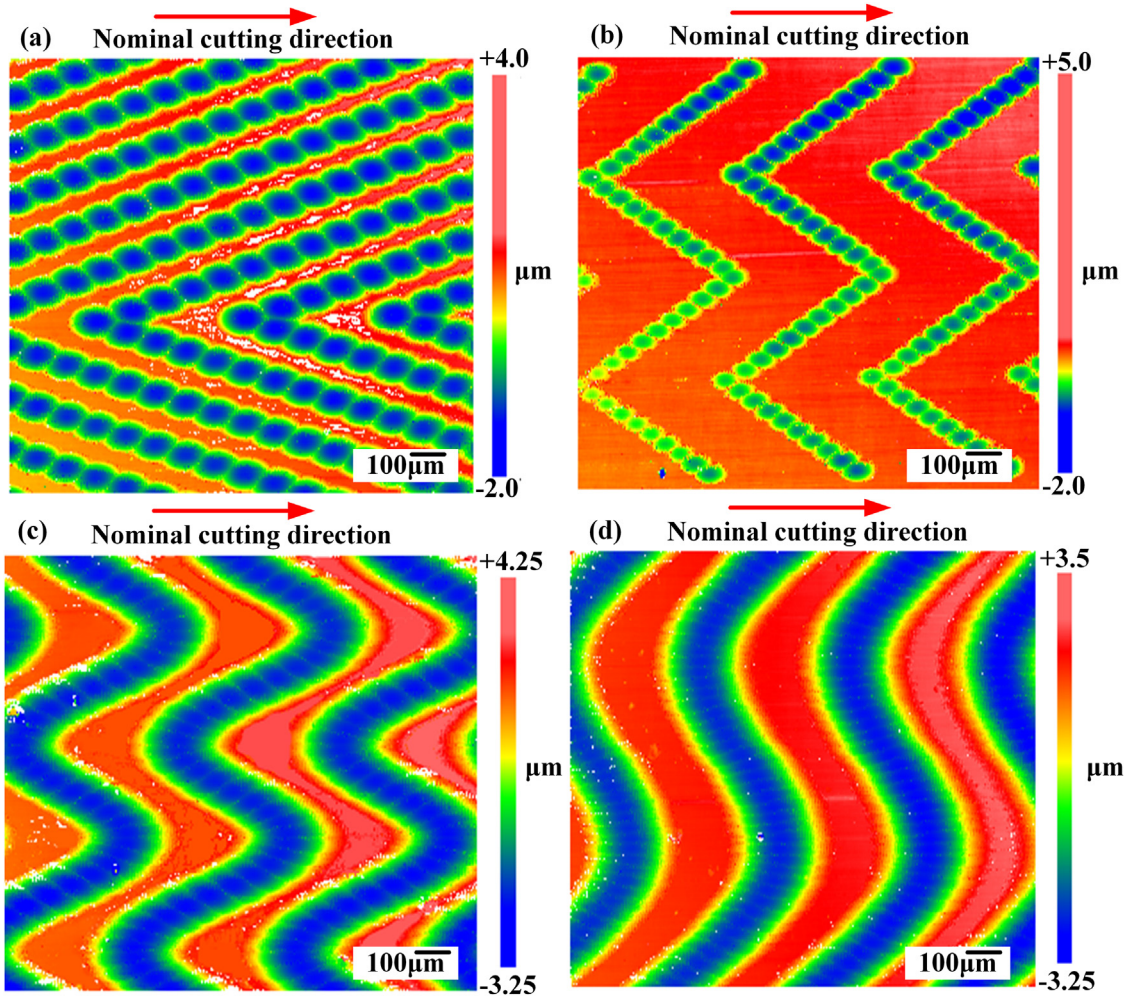

Fig. 14. Surface height maps of generated curving channels (*feed* = 25 μm). (a and b) zigzag curving channels; (c and d) wiggling curving channels.

feature size (due to a larger DOC) to form wiggling microchannels than that to form zigzag microchannels, which results from that the actual DOC (<2 μm) for zigzag microchannels fabrication is smaller than the DOC (>3.8 μm) for wiggling microchannels. Besides, by comparing Fig. 14(c) and (d), we can also find that the boundary of the microchannel with smaller phase-shift distances (Fig. 14(d)) is smoother than that with larger phase-shift distances (Fig. 14(c)). These results and findings are consistent with the analysis with Eq. (4) in section "Generation of hierarchical channels by programming the layout of hierarchical dimples".

Conclusions

This study proposes a flexible and efficient method for the fabrication of hierarchical channels with a controllable cross-section profile and orientation using a modulated vibration texturing process. A low-frequency modulation motion in depth-of-cut (DOC) direction and a high-frequency elliptical vibration are generated simultaneously with a 2-D ultrafast vibration cutting tool. The modulation motion is used to create the primary channels, while the elliptical vibration is used to generate superimposed secondary micro/nanostructures. The following conclusions can be drawn.

(1) A hierarchical dimple is the basic structural unit that the proposed process can fabricate. By programming the layout of hierarchical dimples to control the overlapping of neighboring dimples, hierarchical microchannels with controllable orientations and cross-section profiles can be generated.
(2) The primary channel orientation can be adjusted by tool path planning, while the secondary nanostructures direction can be tuned through the relative angle between the channel formation and nominal cutting direction. In addition, the channel cross-section profile can be de-coupled from the tool geometry but dynamically adjusted through the tool modulation trajectory. For the fabrication of hierarchical microchannels with smoother structural boundary, a larger tool nose radius and larger DOC and smaller feed distance are beneficial.
(3) Based on the kinematics of the cutting tool, numerical simulations have been performed to identify the dependency of geometric parameters of hierarchical microchannel on the process conditions, such as vibration parameters, tool geometries, and cutting parameters. Hierarchical channels with different cross-section profiles and spatial-varying orientations have been fabricated through surface texturing tests to verify the efficacy of the proposed modulated vibration texturing process and the accuracy of numerical simulation.

Declaration of Competing Interest

The authors declare that they have no known competing financial interests or personal relationships that could have appeared to influence the work reported in this paper.

Acknowledgments

This research was supported by the start-up fund from McCormick School of Engineering, Northwestern University, Evanston, IL, USA; and the Innovation and Technology Fund, Hong Kong, #ITS/076/17. This work utilized Northwestern University Micro/Nano Fabrication Facility (NUFAB), which is supported by the State of Illinois and Northwestern University.

References

[1] Malshe, A.P., Bapat, S., Rajurkar, K.P., Haitjema, H., 2018, Bio-inspired textures for functional applications. CIRP Ann – Manuf Technol, 67/2: 627–650.
[2] Chen, H., Ran, T., Gan, Y., Zhou, J., Zhang, Y., Zang, L., et al, 2018, Ultrafast water harvesting and transport in hierarchical microchannels. Nat Mater, 17/10: 935–942.
[3] Tian, Y., Zhu, P., Tang, X., Zhou, C., Wang, J., Kong, T., et al, 2017, Large-scale water collection of bioinspired cavity-microfibers. Nat Commun, 8/1: 1–9.
[4] Lin, G., Zhang, Q., Lv, C., Tang, Y., Yin, J., 2018, Small degree of anisotropic wetting on self-similar hierarchical wrinkled surfaces. Soft Matter, 14/9: 1517–1529.
[5] Tang, Y., Fu, T., Liu, Q., Luo, W., 2015, Copper based superhydrophobic microchannels: fabrication and its effect on friction reduction. Mater Sci Technol, 31/6: 730–736.
[6] Radha, B., Lim, S.H., Saifullah, M.S., Kulkarni, G.U., 2013, Metal hierarchical patterning by direct nanoimprint lithography. Sci Rep, 3/1: 1–8.
[7] Alamri, S., Aguilar-Morales, A.I., Lasagni, A.F., 2018, Controlling the wettability of polycarbonate substrates by producing hierarchical structures using direct laser interference patterning. Eur Polym J, 99:27–37.
[8] Liu, Y., Yin, X., Zhang, J., Wang, Y., Han, Z., Ren, L., 2013, Biomimetic hydrophobic surface fabricated by chemical etching method from hierarchically structured magnesium alloy substrate. Appl Surf Sci, 280:845–849.
[9] Chen, W., Zheng, L., Xie, W., Yang, K., Huo, D., 2019, Modelling and experimental investigation on textured surface generation in vibration-assisted micro-milling. J Mater Process Technol, 266:339–350.
[10] Rodríguez, P., Labarga, J.E., 2013, A new model for the prediction of cutting forces in micro-end-milling operations. J Mater Process Technol, 213/2: 261–268.
[11] Zhu, Z., To, S., Tong, Z., Zhuang, Z., Jiang, X., 2018, Modulated diamond cutting for the generation of complicated micro/nanofluidic channels. Precis Eng, 56:136–142.
[12] Wang, J., Liao, W.H., Guo, P., 2019, Modulated ultrasonic elliptical vibration cutting for ductile-regime texturing of brittle materials with 2-D combined resonant and non-resonant vibrations. Int J Mech Sci, 105347.
[13] Zhou, X., Zuo, C., Liu, Q., Lin, J., 2016, Surface generation of freeform surfaces in diamond turning by applying double-frequency elliptical vibration cutting. Int J Mach Tools Manuf, 104:45–57.
[14] Geng, D., Liu, Y., Shao, Z., Zhang, M., Jiang, X., Zhang, D., 2020, Delamination formation and suppression during rotary ultrasonic elliptical machining of CFRP. Compos Part B: Eng, 183:107698.
[15] Geng, D., Liu, Y., Shao, Z., Lu, Z., Cai, J., Li, X., 2019, Delamination formation, evaluation andsuppression during drilling of composite laminates: a review. Compos Struct, 216:168–186. http://dx.doi.org/10.1016/j.compstruct.2019.02.099.
[16] Wang, J., Du, H., Gao, S., Yang, Y., Zhu, Z., Guo, P., 2019, An ultrafast 2-D non-resonant cutting tool for texturing micro-structured surfaces. J Manuf Process, 48:86–97.
[17] Guo, P., Ehmann, K.F., 2013, An analysis of the surface generation mechanics of the elliptical vibration texturing process. Int J Mach Tools Manuf, 64:85–95.